PHYSICAL REVIEW B **80**, 140511(R) (2009)

Coexistence of incommensurate magnetism and superconductivity in $Fe_{1+y}Se_xTe_{1-x}$

R. Khasanov,[1,*] M. Bendele,[1,2] A. Amato,[1] P. Babkevich,[3,4] A. T. Boothroyd,[3] A. Cervellino,[5] K. Conder,[6] S. N. Gvasaliya,[4] H. Keller,[2] H.-H. Klauss,[7] H. Luetkens,[1] V. Pomjakushin,[4] E. Pomjakushina,[6] and B. Roessli[4]

[1]*Laboratory for Muon Spin Spectroscopy, Paul Scherrer Institute, CH-5232 Villigen PSI, Switzerland*

[2]*Physik-Institut der Universität Zürich, Winterthurerstrasse 190, CH-8057 Zürich, Switzerland*

[3]*Department of Physics, Clarendon Laboratory, Oxford University, Oxford OX1 3PU, United Kingdom*

[4]*Laboratory for Neutron Scattering, Paul Scherrer Institute and ETH Zürich, CH-5232 Villigen PSI, Switzerland*

[5]*Swiss Light Source, Paul Scherrer Institute, CH-5232 Villigen, Switzerland*

[6]*Laboratory for Developments and Methods, Paul Scherrer Institute, CH-5232 Villigen PSI, Switzerland*

[7]*IFP, TU Dresden, D-01069 Dresden, Germany*

(Received 20 July 2009; revised manuscript received 24 August 2009; published 26 October 2009)

We have studied the superconducting and magnetic properties of $Fe_{1+y}Se_xTe_{1-x}$ single crystals ($0 \leq x \leq 0.5$) by magnetic susceptibility, muon-spin rotation, and neutron diffraction. We find three regimes of behavior: (i) commensurate magnetic order for $x \lesssim 0.1$, (ii) bulk superconductivity for $x \sim 0.5$, and (iii) a range $x \approx 0.25-0.45$ in which superconductivity coexists with incommensurate magnetic order. The results are qualitatively consistent with two-band mean-field models in which itinerant magnetism and extended *s*-wave superconductivity are competing order parameters.

DOI: 10.1103/PhysRevB.80.140511 PACS number(s): 74.70.−b, 74.25.Jb, 61.05.F−, 76.75.+i

The recently discovered Fe-based high-temperature superconductors (HTS) host an intriguing competition between magnetic, structural, and superconducting phases. The parent phases, such as *Ln*FeAsO (*Ln*1111, *Ln*=La,Ce,Pr,Sm,...) (Refs. 1–10) and AFe_2As_2 (*A*122, *A*=Ba,Sr,Ca,...) (Refs. 11–15), exhibit commensurate static magnetic order. Upon doping or application of pressure (chemical or mechanical), magnetism is suppressed and superconductivity emerges in a manner that depends on the material. Experiments on fluoride-doped La1111 and Pr1111 indicate that the transition from the superconducting to the magnetic state is of the first order.[3,7] Ce1111 shows a behavior that is more consistent with a quantum-critical point separating magnetic and superconducting states.[5] The experiments on Sm1111 and *A*122 demonstrate the coexistence of magnetism and superconductivity.[9,10,12,16,17]

Recently, Sales *et al.*[18] reported the synthesis of large single crystals of $Fe_{1+y}Se_xTe_{1-x}$ ($0 \leq x \leq 0.5$) belonging to the 011 family of Fe-based HTS. Resistivity measurements showed traces of superconductivity at $T \lesssim 14$ K for all $x \neq 0$ crystals, while bulk superconductivity was detected only for compositions close to $x=0.5$. Nonsuperconducting $Fe_{1+y}Te$ with $y \lesssim 0.1$ exhibits long-range commensurate magnetic order,[19–21] but only short-range incommensurate magnetism survives in Se-doped samples.[20–23] Up to now, however, the relation between the magnetic and superconducting properties has not been studied systematically for the 011 system. Here, we report on a detailed study of $Fe_{1+y}Se_xTe_{1-x}$ single crystals through a combination of magnetic susceptibility, muon-spin rotation (μSR), and neutron diffraction. At the boundary between magnetic and superconducting phases we observe a region of doping in which superconductivity coexists with incommensurate magnetic order. The phase diagram is qualitatively consistent with a two-band itinerant models of the Fe pnictides in which magnetism and extended *s*-wave superconductivity are competing orders.[24,25]

μSR and neutron-diffraction (powder and single crystal) experiments were performed on the πM3 and πE1 beam lines at SμS, and on the HRPT (high resolution powder diffractometer) and TASP (triple-axis spectrometer) instruments at SINQ (all at the Paul Scherrer Institute, Switzerland). ac susceptibility measurements were performed on a Quantum Design PPMS magnetometer with a measuring field $\mu_0 H_{ac}=0.1$ mT and frequency $\nu=1000$ Hz. To reduce the effects of demagnetization thin platelike pieces of $Fe_{1+y}Se_xTe_{1-x}$, cleaved from the main crystals, were oriented with the flat surface (*ab* plane) parallel to the ac field.

Single crystals of $Fe_{1+y}Se_xTe_{1-x}$ were grown by a modified Bridgeman method similar to that reported in Ref. 18. Powders of Fe, Se, and Te of minimum purity 99.99% were mixed in the appropriate ratios, pressed into a rod and vacuum sealed in a double-walled quartz ampule. The rod was first melted and homogenized at 1200 °C for 4 hours and then cooled in a temperature gradient 8 °C/cm at a rate 4 °C/h down to 750 °C followed by 50 °C/h cooling. The crystals had mirrorlike surface and were easily cleaved parallel to the *ab* planes. Several of the crystals were ground into a powder and analyzed by neutron powder diffraction. The amount of the main ($P4/nmm$) fraction was found to be $\simeq$94%, 97%, 98%, and 99% for $x=0.5$, 0.45, 0.4, and 0.25 crystals, respectively. The only impurity phase detected was the hexagonal Fe(SeTe) (space group $P6_3/mmc$).

The ac susceptibility (χ_{ac}) data are shown in Fig. 1. The $x=0.5$ and $x=0.45$ samples are seen to be bulk superconductors with $\chi_{ac}=-1.09$ and -1.18, respectively, at $T \simeq 2$ K. Values of $|\chi_{ac}|$ in excess of unity are likely explained by small nonzero demagnetization factors caused by a slight misalignment of the crystals relative to the direction of the ac field. The $x=0.4$ and 0.25 samples exhibit superconductivity but have a small superconducting fraction of order 10% at low temperature. No trace of superconductivity was detected in the $x=0.1$ and 0.0 samples.

μSR experiments were performed in zero magnetic field

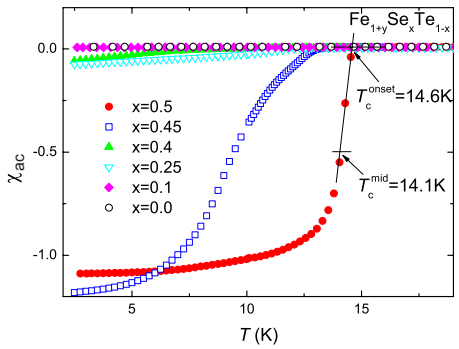

FIG. 1. (Color online) Temperature dependence of the ac volume susceptibility χ_{ac} of $Fe_{1+y}Se_xTe_{1-x}$. The onset T_c^{onset} and the midpoint T_c^{mid} of the superconducting transition are determined from the intersection of straight line fits to the data above and below the transition, and the point corresponding to $\chi_{ac}=-0.5$, respectively.

(ZF), transverse field (TF), and longitudinal field (LF). In TF experiments muons stopping in magnetically ordered parts of the sample lose their polarization rapidly since the magnetic field at the muon stopping site becomes a superposition of the external and the internal fields. ZF experiments provide information on the internal magnetic field distribution, while complementary LF measurements make it possible to discriminate between static and fluctuating fields.

Figure 2 displays μSR results for representative compositions of $Fe_{1+y}Se_xTe_{1-x}$. Figure 2(a) shows that for $x=0.5$ there is no difference between the ZF time spectra measured at $T=1.7$ and 20 K. This suggests that the magnetic state of $FeSe_{0.5}Te_{0.5}$ is the same above and below the superconducting transition temperature. The solid lines correspond to a fit by the function $A^{ZF}(t)=A_0^{ZF}e^{-\Lambda^{ZF}t}$, where A_0^{ZF} is the initial asymmetry and Λ^{ZF} is the exponential relaxation rate. Measurements in LF geometry (not shown) indicate that the exponential character of the muon-spin relaxation is due to randomly oriented local magnetic fields, which are static on the μSR time scale. Such a behavior is consistent with dilute Fe moments as observed recently for another representative of Fe-based HTS $FeSe_{1-x}$.[26] The TF data for $x=0.5$ fit well to the function $A^{TF}(t)=A_0^{TF}e^{-(\Lambda^{TF}t+\sigma^2t^2/2)}\cos(\gamma_\mu Bt+\phi)$. Here, $\gamma_\mu/2\pi=135.5$ MHz/T is the muon gyromagnetic ratio, ϕ is the initial phase of the muon-spin ensemble, and σ is the Gaussian relaxation rate. The right panel of Fig. 2(a) shows that the TF asymmetry A_0^{TF} is almost temperature independent. The slightly stronger relaxation of the muon-spin polarization at 1.7 K relative to 20 K is due to the formation of the vortex lattice at $T<T_c$.

For the $x=0.45$ sample [Fig. 2(b)] there is little change in either the ZF or the TF time spectra on cooling from 20 to ~7 K. At lower temperatures, however, an additional fast relaxing component starts to develop. The solid lines in Fig. 2(b) (left panel) correspond to fits with $A^{ZF}(t)=A_1^{ZF}e^{-\Lambda_1^{ZF}t}+A_2^{ZF}e^{-\Lambda_2^{ZF}t}$ and $A^{TF}(t)=e^{-\sigma^2t^2/2}[A_1^{TF}e^{-\Lambda_1^{TF}t}\cos(\gamma_\mu B_1t+\phi)+A_2^{TF}e^{-\Lambda_2^{TF}t}\cos(\gamma_\mu B_2t+\phi)]$. Here, $A_{1(2)}^{ZF(TF)}$ and $\Lambda_{1(2)}^{ZF(TF)}$ are the initial ZF (TF) asymmetry and the exponential depolarization rate of the slow (fast) relaxing component, respectively. The decrease in A_1^{TF} with

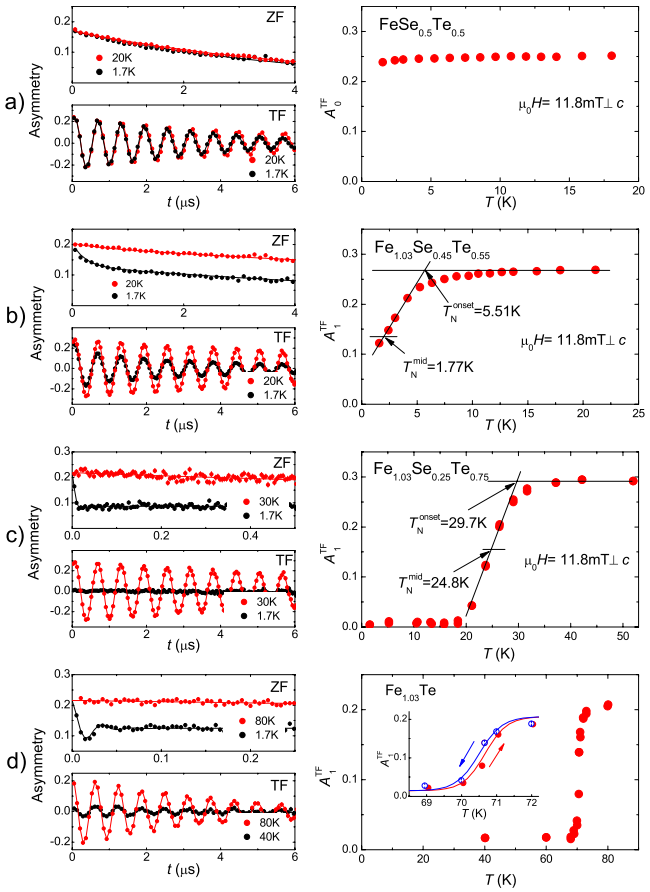

FIG. 2. (Color online) Representative ZF and TF μSR time spectra (left panels) and temperature-dependent initial TF asymmetry of the slow relaxing component (A_0^{TF} and A_1^{TF}, right panels) for single crystals of $Fe_{1+y}Se_xTe_{1-x}$. The onset (T_N^{onset}) and the midpoint (T_N^{mid}) of the magnetic transition are determined from the intersection of straight lines fit to the data above and below the transition and the point where the asymmetry reaches 1/2 of its maximum value, respectively.

decreasing temperature [Fig. 2(b), right panel] is due to the development of magnetic order, which at $T\simeq1.7$ K occupies more than 50% of the whole sample volume. The LF data reveal that the slow relaxing component completely recovers at $\simeq10$ mT (similar to that observed for $x=0.5$), while the asymmetry of the fast relaxing one decreases by ~50% at $B^{LF}=0.4$ T. Since the muon spins become decoupled from the static internal field B_{int} at $B^{LF}\gtrsim10B_{int}$,[27] we may assume that the magnetism that develops in the $x=0.45$ sample below $T\approx7$ K is caused by the static internal field $B_{int}\gtrsim0.1$ T at the muon stopping site.

Magnetism was found to develop in the $x=0.4$, 0.25, 0.1, and 0.0 samples below $T\simeq18$, 30, 40, and 70 K, respectively, as signaled by a fast drop of both A^{ZF} and A^{TF} within the first 100 ns [see Figs. 2(c) and 2(d); the ZF and TF time spectra for $x=0.4$ and $x=0.1$ look very similar to that of the $x=0.25$ sample and are not shown]. The TF and ZF data for $x=0.4$, 0.25, and 0.1 were fitted similarly to $x=0.45$. In order to fit the highly damped oscillations observed for $x=0$ [Fig. 2(d)] the second term in $A^{ZF}(t)$ was multiplied by $\cos(\gamma_\mu B_{int}t)$. This sample shows an abrupt change in

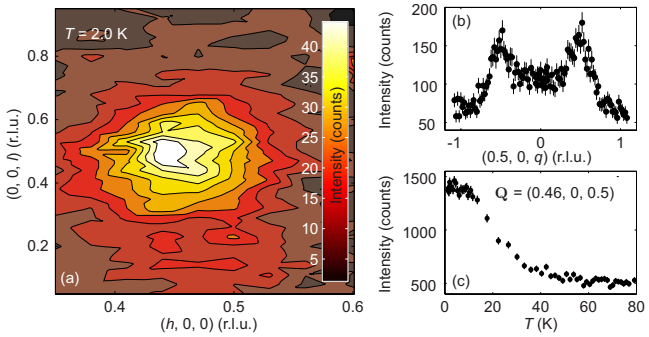

FIG. 3. (Color online) Neutron diffraction from $Fe_{1.03}Se_{0.25}Te_{0.75}$. (a) Intensity of spin-flip scattered polarized neutrons in the $(h,0,l)$ plane. (b) **Q** scan through the magnetic peaks. (c) Temperature dependence of the intensity at (0.46,0,0.5) measured with unpolarized neutrons.

$B_{\rm int} \simeq 0.21$ T at $T \simeq 70.6$ K and hysteresis in $A_1^{\rm TF}(T)$ measured on increasing and decreasing temperature [see inset in the right panel of Fig. 2(d)]. These features are evidence for a first-order magnetic transition in $Fe_{1.03}Te$, which is consistent with the results of Refs. 20 and 21. To within our experimental accuracy there is no hysteresis in the magnetic transition for the $x=0.45$, 0.4, 0.25, and 0.1 samples.

The fact that the ZF time spectra for the $x=0$ sample can be well described by a damped cosine function with *zero* initial phase [see Fig. 2(d)] suggests that the magnetism in $Fe_{1.03}Te$ is commensurate.[28] The absence of ZF oscillations for samples with $x>0$ prevents any firm conclusions being drawn about the type of magnetism in these samples. To learn how the magnetic correlations change with Se doping, we performed neutron-diffraction measurements on the $x=0.25$ crystal. The neutron polarization analysis device MuPAD (Ref. 29) was employed to separate magnetic from nonmagnetic scattering. Figure 3(a) is a color map of the spin-flip (SF) scattering in the $(h,0,l)$ plane in the reciprocal space (referred to the tetragonal unit cell with $a \simeq 3.8$ Å and $c \simeq 6.2$ Å).[21] The sample temperature was 2 K, and the neutron wavelength was 3.2 Å. The neutron polarization **P** was maintained parallel to the scattering vector **Q**, so that the SF scattering is purely magnetic. The map reveals a magnetic peak centered on the incommensurate wave vector (0.46,0,0.5). Figure 3(b) shows a scan along $\mathbf{Q}=(0.5,0,l)$, i.e., displaced slightly from the peak center. Two magnetic Bragg peaks with equal intensities are observed. The peaks are broader than expected from the resolution of the spectrometer and correspond to correlation lengths of $\xi_a = 11.5 \pm 1.0$ Å and $\xi_c = 6.0 \pm 0.5$ Å. Additional Bragg peaks were found at $(0.46,0,-1.5)$, $(1.46,0,-1.5)$, and $(0.46,0,-2.5)$, corresponding to a magnetic arrangement described by the propagation vector $\mathbf{k}=(0.46,0,\pm 0.5)$.

Figure 3(c) shows the temperature dependence of the peak intensity at (0.46,0,0.5) measured with unpolarized neutrons. The magnetic peak emerges below $T \approx 40$ K, which is consistent with the muon asymmetry data [Fig. 2(c)]. A recent study on a crystal of $Fe_{1.07}Se_{0.25}Te_{0.75}$ has also reported incommensurate magnetic order.[22] The incommensurate peaks were observed on one side of the AFM wave vector and were explained in terms of an imbalance of ferromagnetic/antiferromagnetic correlations between nearest-neighbor spins. The incommensurability and ξ_c are consistent with our results, but ξ_a is a factor of 2 smaller than in our sample.

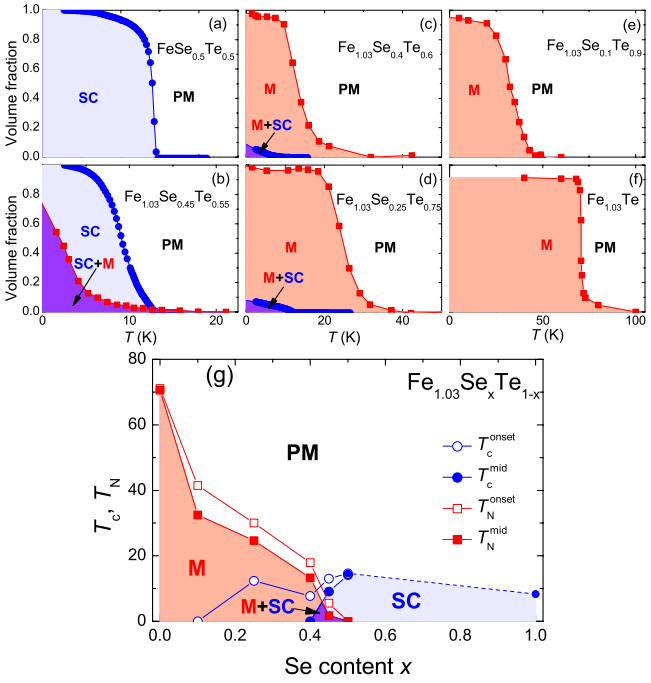

FIG. 4. (Color online) (a)–(f) Temperature dependence of the superconducting (SC) and magnetic (M) volume fractions in $Fe_{1.03}Se_xTe_{1-x}$. PM denotes the paramagnetic phase. (g) Phase diagram showing $T_c^{\rm onset}$, $T_c^{\rm mid}$, $T_N^{\rm onset}$, and $T_N^{\rm mid}$ as functions of x. The datum for $FeSe_{1-x}$ is from Ref. 26.

Figure 4 summarizes our results on the magnetism and superconductivity in $Fe_{1+y}Se_xTe_{1-x}$. The volume fraction curves for the superconducting (SC) and magnetic (M) phases are taken from $\chi_{\rm ac}(T)$ (Fig. 1) and $A_1^{\rm TF}(T)$ (Fig. 2), respectively. The latter represents the fraction of muons experiencing a static local field. Figure 4(g) shows the midpoint and the onset of the superconducting and magnetic transitions, determined as shown in Figs. 1 and 2, as functions of x. It can be seen that superconductivity occurs throughout the bulk of the $x=0.45$ and 0.5 crystals, while it occupies up to $\simeq 10\%$ of the sample volume in the $x=0.25$ and $x=0.4$ samples as $T \to 0$. Magnetic order is present in the $x=0.45$, 0.4, 0.25, 0.1, and 0.0 samples with respective volume fractions of $\simeq 75\%$, 98%, 98%, 95%, and 92% at $T \to 0$.

Most interestingly, superconductivity and magnetism are shown to coexist within certain temperature ranges in the $x=0.45$, 0.4, and 0.25 samples. For $x=0.45$, magnetism starts to develop below the superconducting transition temperature [Fig. 4(b)], while in $x=0.4$ and 0.25 magnetism appears first and superconductivity emerges at a lower temperature [Figs. 4(c) and 4(d)]. The data do not show any evidence that one form of order emerges at the expense of the other, for if that were the case then a growth in one order parameter would coincide with a decrease in the other. This is clearly not the case as may be seen in Figs. 4(b)–4(d). Nor do the data provide any evidence for macroscopic phase separation into superconducting and magnetic clusters (bigger than a few

nm in size), as observed e.g., for $Ba_{1-x}K_xFe_2As_2$.[16] In such a case the sum of magnetic and superconducting volume fractions at a given T should never exceed unity as they do here, especially for $x=0.45$.

To account for the coexistence of superconductivity and magnetism in $Fe_{1+y}Se_xTe_{1-x}$, we consider two scenarios. The first is a *nanoscale* segregation into magnetic domains, similar to that reported for cuprate HTS.[28,30,31] In underdoped cuprate HTS, static, short-range, and stripelike magnetic correlations are thought to exist in the superconducting state and are assumed not to affect the superconducting carriers.[30] Muons are sensitive to dipolar fields at a distance of up to a few lattice spacings, so if nanoscale magnetic domains exist then the fraction of muons experiencing static local magnetic fields could be significantly higher than the fraction of Fe sites carrying an ordered moment. On the other hand, no evidence has been found yet for local magnetic domains in Fe-based compounds. In fact, a recent nuclear magnetic resonance study of $Ba(Fe_{1-x}Co_x)_2As_2$ showed the appearance of magnetic order on *all* Fe sites thus ruling out nanoscale segregation in that material.[17]

The second possibility is a coexistence of the two order parameters on the *atomic* scale. The combination of incommensurate magnetism and superconductivity is compatible with models recently proposed in Refs. 24 and 25. According to Ref. 24, when $T_N^0/T_c^{max} \sim 1$, where T_N^0 is the magnetic ordering temperature at zero doping ($x=0$) and T_c^{max} is the maximum value of the of the superconducting transition temperature for a given family of Fe-based HTS, the magnetic order is commensurate and the transition between the magnetic and superconducting phases with x is first order. However, for larger T_N^0/T_c^{max} the transition between commensurate magnetic order and superconductivity goes through a region of x where superconductivity coexists with incommensurate magnetic order. In the series $Fe_{1+y}Se_xTe_{1-x}$ studied here we find just such a behavior. It is a commensurate magnet without superconductivity at $x=0$ and a nonmagnetic superconductor at $x=0.5$. In between, at $x=0.25$, we observe incommensurate magnetism coexistent with $\sim 10\%$ superconducting fraction. These results are encouraging for the model, but details still need to be worked out. For example, both $LaFeAsO_xF_{1-x}$ and $Fe_{1+y}Se_xTe_{1-x}$ have $T_N^0/T_c^{max} \simeq 5$, yet $LaFeAsO_xF_{1-x}$ apparently exhibits a first-order transition between magnetic and superconducting phases as a function of x without an intermediate region of coexistence.[3]

In conclusion, the phase diagram of $Fe_{1+y}Se_xTe_{1-x}$ bears a strong resemblance to that of other iron pnictide superconductors, but the existence of an intermediate range of doping in which superconductivity coexists with incommensurate magnetic order appears to be specific to $Fe_{1+y}Se_xTe_{1-x}$. The existence of such a phase has been predicted theoretically and is of particular interest in view of the possibility of a Fulde-Ferrell-Larkin-Ovchinnikov state.[25]

This work was performed at the SμS and SINQ, Paul Scherrer Institute (PSI, Switzerland). M.B. was supported by the Swiss National Science Foundation, and E.P. was supported by the NCCR program MaNEP. A.T.B. thanks the PSI for support during an extended visit in 2009. R.K. thanks A. B. Vorontsov for helpful discussions.

*rustem.khasanov@psi.ch

[1] C. de la Cruz *et al.*, Nature (London) **453**, 899 (2008).
[2] H.-H. Klauss *et al.*, Phys. Rev. Lett. **101**, 077005 (2008).
[3] H. Luetkens *et al.*, Nature Mater. **8**, 305 (2009).
[4] G. F. Chen *et al.*, Phys. Rev. Lett. **100**, 247002 (2008).
[5] J. Zhao *et al.*, Nature Mater. **7**, 953 (2008).
[6] J. Zhao *et al.*, Phys. Rev. B **78**, 132504 (2008).
[7] C. Rotundu *et al.*, Phys. Rev. B **80**, 144517 (2009).
[8] J. P. Carlo *et al.*, Phys. Rev. Lett. **102**, 087001 (2009).
[9] A. J. Drew *et al.*, Nature Mater. **8**, 310 (2009).
[10] S. Sanna *et al.*, Phys. Rev. B **80**, 052503 (2009).
[11] A. Jesche *et al.*, Phys. Rev. B **78**, 180504(R) (2008).
[12] A. A. Aczel *et al.*, Phys. Rev. B **78**, 214503 (2008).
[13] Q. Huang *et al.*, Phys. Rev. Lett. **101**, 257003 (2008).
[14] J. Zhao *et al.*, Phys. Rev. B **78**, 140504(R) (2008).
[15] A. I. Goldman *et al.*, Phys. Rev. B **78**, 100506(R) (2008).
[16] J. T. Park *et al.*, Phys. Rev. Lett. **102**, 117006 (2009).
[17] Y. Laplace *et al.*, Phys. Rev. B **80**, 140501(R) (2009).
[18] B. C. Sales *et al.*, Phys. Rev. B **79**, 094521 (2009).
[19] D. Fruchart *et al.*, Mater. Res. Bull. **10**, 169 (1975).
[20] S. Li *et al.*, Phys. Rev. B **79**, 054503 (2009).
[21] W. Bao *et al.*, Phys. Rev. Lett. **102**, 247001 (2009).
[22] J. Wen *et al.*, Phys. Rev. B **80**, 104506 (2009).
[23] M. Lumsden *et al.*, arXiv:0907.2417 (unpublished).
[24] A. B. Vorontsov *et al.*, Phys. Rev. B **79**, 060508(R) (2009).
[25] V. Cvetkovic and Z. Tesanovic, Phys. Rev. B **80**, 024512 (2009).
[26] R. Khasanov *et al.*, Phys. Rev. B **78**, 220510(R) (2008).
[27] A. Schenck, *Muon Spin Rotation: Principles and Applications in Solid State Physics* (Adam Hilger, Bristol, 1986).
[28] A. T. Savici *et al.*, Phys. Rev. B **66**, 014524 (2002).
[29] M. Janoschek *et al.*, Physica B **397**, 125 (2007).
[30] S. Sanna *et al.*, Phys. Rev. Lett. **93**, 207001 (2004).
[31] P. L. Russo *et al.*, Phys. Rev. B **75**, 054511 (2007).